ACS AUTHORCHOICE
Review

Environmental Science & Technology Letters

pubs.acs.org/journal/estlcu

Sealing Shales versus Brittle Shales: A Sharp Threshold in the Material Properties and Energy Technology Uses of Fine-Grained Sedimentary Rocks

Ian C. Bourg*

Department of Civil and Environmental Engineering and Princeton Environmental Institute, Princeton University, E-208 E-Quad, Princeton, New Jersey 08544, United States

Supporting Information

ABSTRACT: Fine-grained sedimentary rocks (shale and mudstone) play important roles in global CO_2 abatement efforts through their uses in carbon capture and storage (CCS), radioactive waste storage, and shale gas extraction. These different technologies, however, rely on seemingly conflicting premises regarding the sealing properties of shale and mudstone, suggesting that those rocks that lend themselves to hydrocarbon extraction may not be optimal seals for CCS or radioactive waste storage, and vice versa. In this paper, a compilation of experimental data on the properties of well-characterized shale and mudstone formations is used to demonstrate that clay mineral mass fraction, X_{clay}, is a very important variable the controls key material properties of these formations and that a remarkably sharp threshold at $X_{clay} \sim {}^{1}/_{3}$ separates fine-grained rocks with very different properties. This threshold coincides with the predictions of a simple conceptual model of the microstructure of sedimentary rocks and is reflected in the uses of shale and mudstone formations for CCS, radioactive waste storage, and shale gas extraction.

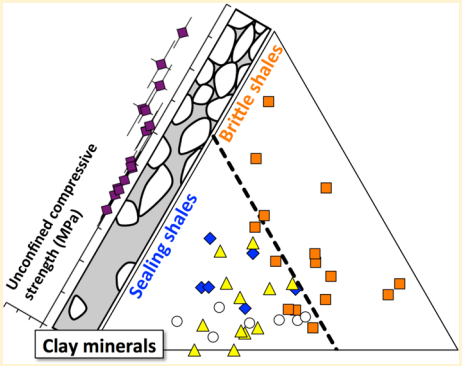

INTRODUCTION

Fine-grained sedimentary rocks (hereafter termed shales and mudstones) account for roughly two-thirds of the sedimentary rock mass.[1,2] Vast formations of these rocks play important roles in three low-carbon energy technologies that have the potential to contribute up to 70% of global CO_2 abatement efforts required to stabilize atmospheric CO_2 levels over the next half-century (Figure 1).[3,4] In carbon capture and storage (CCS), shale and mudstone are the predominant lithologies used or considered for use as caprocks of geologic CO_2 storage sites.[4,5] In nuclear energy production, they constitute a promising option for isolating radioactive waste on time scales greater than the half-lives of long-lived radioactive fission products.[6] Finally, the transition from coal to natural gas as an energy source in North America is driven largely by hydrocarbons extracted from fine-grained sedimentary rocks.[7] These multiple emerging roles of shale and mudstone have prompted concerns about the allocation of these rocks between hydrocarbon extraction, CCS, and nuclear waste storage.[8]

The technologies listed above rely on the ability of fine-grained sedimentary rocks to essentially immobilize fluids (water, CO_2, and hydrocarbons) in the subsurface. Chemical, isotopic, and fluid pressure gradients across shale and mudstone formations indicate that these rocks, at least in some cases, maintain their very low permeability (on the order of 10^{-20} m^2 in core-scale laboratory experiments) over length scales of hundreds of meters and time scales of millions of years.[6,9] Utilization of shale and mudstone in CCS and radioactive waste

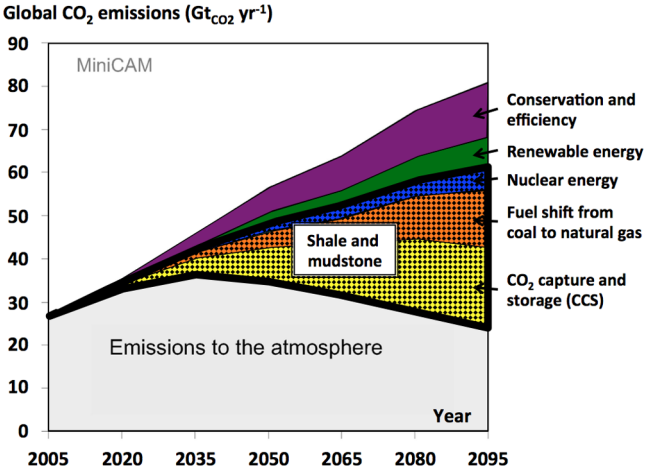

Figure 1. Contribution of different low-carbon energy technologies to global CO_2 emission reductions over the next century according to one scenario proposed by the Intergovernmental Panel on Climate Change (IPCC). The checkered area highlights the technologies that rely on shale and mudstone. Figure modified from ref 4.

Received: July 9, 2015
Accepted: September 9, 2015
Published: September 9, 2015

DOI: 10.1021/acs.estlett.5b00233
Environ. Sci. Technol. Lett. 2015, 2, 255−259

Figure 2. Approximate locations of the shale and mudstone formations compiled in this study. Colors indicate current uses or proposed uses of these formations: orange, unconventional hydrocarbon extraction; yellow, CCS; blue, radioactive waste storage; white, other.

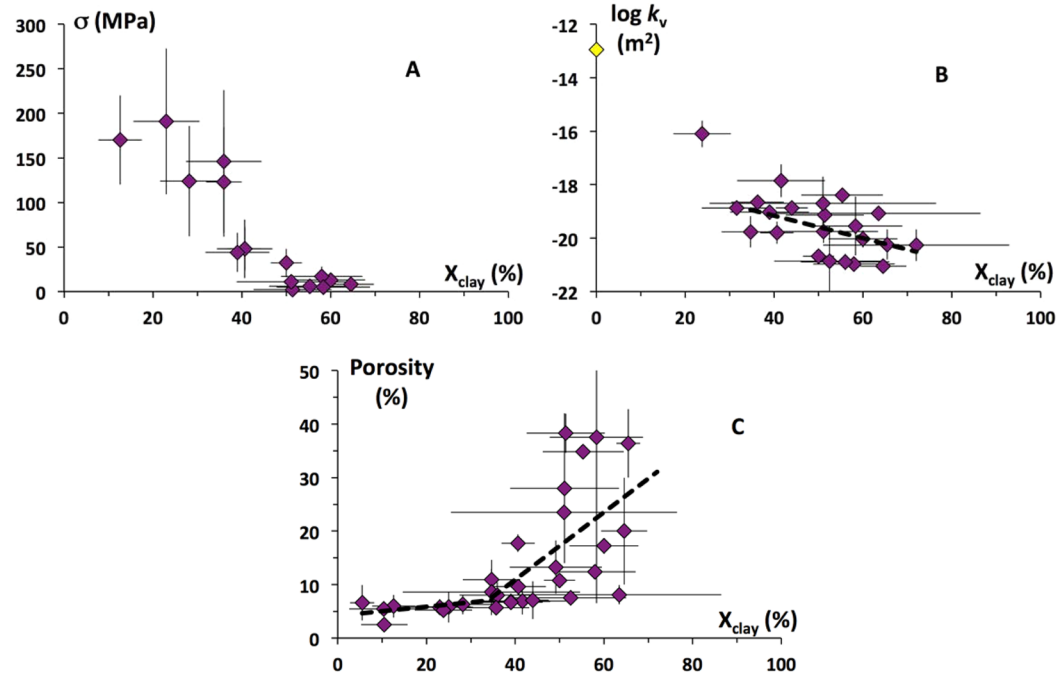

Figure 3. Experimental data on the core-scale unconfined compressive strength (σ), vertical permeability (k_v), and porosity (ϕ) of shale and mudstone as a function of clay mineral mass fraction (X_{clay}). The dashed lines are linear fits to the data at $X_{clay} < 35\%$ ($\phi = 4.2 + 0.08X_{clay}$) and $X_{clay} > 35\%$ ($\phi = -14.2 + 0.63X_{clay}$; $\log k_v = -17.5 - 0.042X_{clay}$). In panel B, the yellow symbol at $X_{clay} = 0$ and $k_v = 10^{-12.95\pm0.63}$ m^2 describes the permeability of generic sandstone with 10% porosity.[21,22]

storage requires, additionally, that the sealing properties of these rocks be resilient to the formation of fractures.[10,11] Extraction of hydrocarbons from fine-grained rocks relies on the opposite premise that permeability can be significantly enhanced, for durations of years or more, by the formation of hydraulic fractures.[12] This contrast suggests that fine-grained rocks that lend themselves to hydrocarbon extraction may not be optimal seals for CCS or radioactive waste storage, and vice versa.

With the emergence of shale and mudstone as key players in CCS, radioactive waste storage, and unconventional hydrocarbon extraction, a significant number of formations have now been extensively characterized. Table S1 of the Supporting Information presents a compilation of the available experimental database. The compilation includes data on the

DOI: 10.1021/acs.estlett.5b00233
Environ. Sci. Technol. Lett. 2015, 2, 255−259

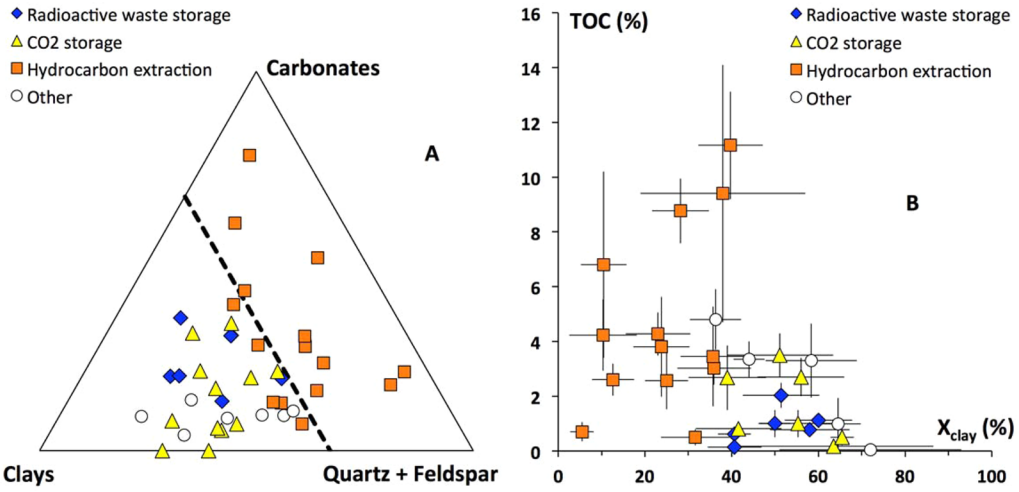

Figure 4. Experimental results on the mineralogy of well-characterized shale and mudstone formations. (A) Ternary diagram showing the three main types of minerals present in shale: phyllosilicates (clay minerals), tectosilicates (quartz and feldspar), and other minerals (primarily carbonates). (B) Plot of total organic carbon (TOC) content as a function of phyllosilicate content (X_{clay}). Colors indicate the current uses or proposed uses of each shale formation: orange, hydrocarbon extraction; yellow, CCS; blue, radioactive waste storage; white, other. The dashed line in panel A indicates rocks with $X_{clay} = {}^1/_3$.

mineralogy [expressed as the fraction of clay minerals, X_{clay}, quartz and feldspars, X_{QF}, and other minerals (primarily carbonates), X_{CO_3}], total organic carbon (TOC), total porosity (ϕ), permeability normal to bedding (k_v), unconfined compressive strength (σ), and uses or proposed uses of 42 well-characterized shale and mudstone formations across North America, Europe, Asia, and Australia (Figure 2).

RESULTS AND DISCUSSION

Experimental data on the properties of well-characterized shales and mudstones reveal evidence of a threshold in unconfined compressive strength (σ) at a phyllosilicate (clay mineral) mass fraction $X_{clay} \sim {}^1/_3$, where rock strength decreases by a factor of 20 (Figure 3A). This transition is highly relevant to the self-sealing of shale and mudstone fractures, because σ may constitute a reasonable proxy for the stresses necessary to crush asperities, or the proppants used in hydraulic fracturing, into a rock surface.[13] Experiments with fractured shale suggest that minor amounts of shearing can result in a 6 order of magnitude decrease in fracture permeability if the effective normal stress (the difference between confining stress and fluid pressure in the direction normal to the fracture) is greater than the σ value of the rock.[13] The existence of a threshold at $X_{clay} \sim {}^1/_3$ in unconfined compressive strength is consistent with a recent observation that the mechanics of fracture slip (gouge dilantancy, frictional strength, and stability) in core samples from three shale formations undergo a transition at $X_{clay} \sim 30\%$.[14]

Experimental data on the core-scale vertical permeability (k_v) and porosity (ϕ) of fine-grained sedimentary rocks provide additional evidence that X_{clay} is a very important rock property and that a threshold may exist at $X_{clay} \sim {}^1/_3$. In particular, the log k_v values of fine-grained rocks are well-known to be much more sensitive to X_{clay} than to ϕ or other variables.[15] Existing data reveal that k_v decreases by 6 orders of magnitude as X_{clay} increases from 0 to 35% and by an additional 1.5 orders of magnitude as X_{clay} increases from 35 to 70% (Figure 3B). The possible threshold at $X_{clay} \sim {}^1/_3$ in Figure 3B is even more sharply pronounced in measurements of the permeability of homogeneous quartz/clay mixtures,[16] but it is absent in field-scale reconstructions of fault permeability versus fault clay content,[17,18] a difference attributed to the scale dependence of permeability in heterogeneous porous media.[17] Similarly, porosity ϕ has little dependence on clay content at $X_{clay} < {}^1/_3$ and a much larger dependence above this threshold (Figure 3C). The evidence of a possible threshold in Figure 3C is remarkable, because the ϕ values of shale and mudstone are well-known to be highly sensitive to the maximal historical burial depth of the rock formation.[9,15] The much greater scatter in the ϕ values of clay-rich rocks in Figure 3B suggests that the sensitivity of porosity to other variables (maximal burial depth, cementation, and recrystallization)[9,19] increases significantly at $X_{clay} > {}^1/_3$. Porosity and permeability are key variables in basin modeling,[2] in geomechanical predictions of caprock failure in CCS,[20] and in predictions of the sealing properties of faults,[18] but most extant models assume that ϕ and k_v are invariant with X_{clay}.[15] The few models that correctly recognize the impact of X_{clay} on k_v do not account for the existence of a possible threshold at $X_{clay} \sim {}^1/_3$.[2,18]

The transition at $X_{clay} \sim {}^1/_3$ in the unconfined compressive strength of shale and mudstone (Figure 3A) and, perhaps, in other material properties (Figures 3B,C) is reflected in a remarkably sharp mineralogical demarcation between fine-grained sedimentary rocks that are exploited for hydrocarbons and those that are used or considered for use in CCS or radioactive waste storage. The former are clay-poor, while the latter are clay-rich (Figure 4A). The mineralogy of the average shale ($X_{clay} \sim 55$–60%, $X_{QF} \sim 30$–35%, and $X_{CO_3} \sim 4$–9%)[1,23] lies well within the range of compositions that are not amenable to hydrocarbon extraction. The demarcation between different uses shows a minor dependence on the total organic carbon (TOC) content of the shale as shown in Figure 4B. Overall, the results shown in Figure 4 indicate that X_{clay} is a very important variable that controls the utility of shales and mudstones as seals (for CCS or radioactive waste storage) or as hydrocarbon resources.

The existence of a threshold in the properties of shale at $X_{clay} \sim {}^1/_3$ is consistent with a conceptual model of shale

DOI: 10.1021/acs.estlett.5b00233
Environ. Sci. Technol. Lett. 2015, 2, 255–259

microstructure as a mixture of large grains (quartz, feldspar, and carbonates) and a fine-grained clay matrix (Figure 5). On this

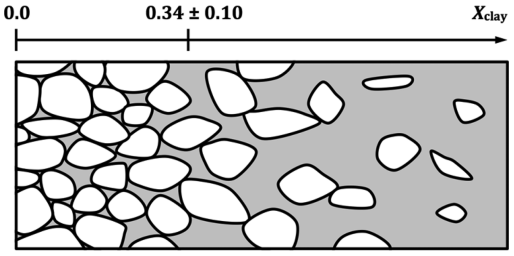

Figure 5. Conceptual model of shale and mudstone microstructure as a mixture of large grains (white) and a fine-grained clay matrix (gray). Quartz, feldspar, and carbonate grains in shale and mudstone have dimensions on the order of $\sim 10^{-5}$ to 10^{-4} m, whereas clay minerals have dimensions on the order of 10^{-8} to 10^{-7} m. The clay mineral mass fraction increases from left to right. On the left side of the figure, the large grains from a load-bearing network. On the right side, the clay matrix is the load-bearing phase. If the large grains are spherical and monodisperse, the transition between the two conditions should occur at $X_{clay} = 0.34 \pm 0.10$. Figure modified from ref 16.

model, a threshold value of X_{clay} naturally arises where the fine-grained clay matrix optimally fills the space between the larger grains.[16] This threshold value of X_{clay} is determined by the relation

$$X_{clay,threshold} = \{1 + (\rho_{s,grains} f_{grains})/[\rho_{b,clay}(1 - f_{grains})]\}^{-1} \quad (1)$$

where f_{grains} is the volumetric packing density of the large grains of quartz, feldspar, or calcite, $\rho_{s,grains}$ is the solid density of the large grains, and $\rho_{b,clay}$ is the dry bulk density of the clay matrix. The values of the parameters in eq 1 can be estimated as $\rho_{b,clay} = 2.01 \pm 0.85$ kg dm^{-3} (the solid density of muscovite mica, 2.83 kg dm^{-3},[24] multiplied by a factor of 0.71 ± 0.3, calculated on the basis of the ϕ values compiled in Figure 3C, to account for the porosity of the clay matrix), $\rho_{s,grains} = 2.67 \pm 0.07$ kg dm^{-3} (the average of the mineral grain densities of quartz, feldspar, and calcite),[24] and $f_{grains} = 0.595 \pm 0.035$ (the experimental range for monodisperse spheres settled, dropped, or poured into a bed).[25] This yields $X_{clay} = 34 \pm 10\%$, where the confidence interval primarily reflects the uncertainty of the porosity of the clay matrix. If X_{clay} is smaller than the threshold value, the large grains form a load-bearing framework and the clay matrix partially fill the space between the grains. If X_{clay} is greater than the threshold value, the clay matrix is the load-bearing phase (Figure 5). The coincidence of the predicted and observed thresholds strongly suggests that a very simple aspect of shale microstructure, the manner in which the clay matrix fills the space between larger grains, controls the core-scale fluid flow and mechanical properties of shales and mudstones (Figure 3) and the uses of these rocks (Figure 4). This coincidence is all the more remarkable in light of the extreme simplicity of the conceptual model used to derive eq 1, which neglects the heterogeneity of real rocks, the effect of cementation and recrystallization, and the nonspherical, non-monodisperse nature of large mineral grains.

One prediction of the conceptual model in Figure 5 is that in the case of shale or mudstone fractures exposed to a compressive effective normal stress, surface asperities or exogenous proppants will be supported by a network of large grains in the underlying rock matrix if $X_{clay} < {}^1/_3$. Therefore, fractured shales and mudstones should have a much greater tendency to self-seal in the presence of compressive effective normal stresses if $X_{clay} > {}^1/_3$. Self-sealing of fractures has in fact been observed in the case of the clay-rich rocks considered for use in CCS and radioactive waste storage.[10,13] The coincidence of the thresholds in Figures 3A, 4A, and 5 supports the use of σ as a proxy for the ability of the rock matrix to support asperities or proppants.[13]

Another prediction of the conceptual model in Figure 5 is that the mechanics of shale and mudstone fractures should be sensitive to geochemical alterations of fracture surface mineralogy by reactive fluids. In CCS, the flow of CO_2/brine mixtures through fractures can cause a rapid dissolution of carbonate minerals on fracture surfaces.[26,27] Previous studies have implied that this phenomenon may impair seal integrity. The work presented here indicates that the dissolution of carbonate minerals may instead improve seal integrity by increasing X_{clay} on fracture surfaces and, therefore, decreasing the normal compressive stresses required to seal fractures. This hypothesis is supported by recent examinations of reactive fluid flow at debonded cement−caprock interfaces.[28,29] For the same reason, this work suggests that the use of acidic fluids in the stimulation of hydraulic fractures may have a deleterious effect on shale hydrocarbon extraction, as observed experimentally,[30] by increasing X_{clay} on fracture surfaces.

Finally, the conceptual model presented in Figure 5 suggests that thresholds at $X_{clay} \sim {}^1/_3$ may exist in other situations involving fine-grained geologic media. For example, one mechanism of leakage through poorly cemented wells involves the flow of fluid through a gap between the well cement and the rock surface.[28] The study presented here suggests that this type of leakage may be much less likely in wells drilled through rocks with $X_{clay} > {}^1/_3$, with potential implications for efforts to quantify CO_2 or methane emissions from poorly cemented wells.[31] Similarly, this study suggests that the mechanics of fault rupture and slip, known to be sensitive to the clay content of the fault gouge,[32,33] may exhibit a threshold at $\sim {}^1/_3$ clay minerals in the fault gouge.

■ ASSOCIATED CONTENT

Supporting Information

The Supporting Information is available free of charge on the ACS Publications website at DOI: 10.1021/acs.estlett.5b00233.

A table summarizing the experimental data plotted in Figures 3 and 4 (Table SI1) and references (PDF)

■ AUTHOR INFORMATION

Corresponding Author

*Department of Civil and Environmental Engineering, E-208 E-Quad, Princeton University, Princeton NJ 08544; (+1)609-258-4541; bourg@princeton.edu.

Notes

The author declares no competing financial interest.

■ ACKNOWLEDGMENTS

This study was performed under the auspices of the Center for Nanoscale Control of Geologic CO_2, an Energy Frontiers Research Center (EFRC) funded by the U.S. Department of Energy, Office of Science, Office of Basic Energy Sciences, under Award DE-AC02-05CH11231. The author is grateful to Drs. Garrison Sposito, Jeffrey A. Reimer, and Donald J. DePaolo (University of California, Berkeley, CA) for advice on

DOI: 10.1021/acs.estlett.5b00233
Environ. Sci. Technol. Lett. 2015, 2, 255−259

early versions of the manuscript, as well as to Drs. Martin Mazurek (University of Berne), William Arnold (University of Minnesota), and one anonymous reviewer for useful comments on the manuscript.

REFERENCES

(1) Shaw, D. B.; Weaver, C. E. The mineralogical composition of shales. *J. Sediment. Petrol.* **1965**, *35*, 213−222.
(2) Yang, Y.; Aplin, A. C. A permeability-porosity relationship for mudstones. *Mar. Pet. Geol.* **2010**, *27*, 1692−1697.
(3) Pacala, S.; Socolow, R. Stabilization wedges: Solving the climate problem for the next 50 years with current technologies. *Science* **2004**, *305*, 968−972.
(4) IPCC. IPCC Special Report on Carbon Dioxide Capture and Storage. Metz, B., Davidson, O., de Coninck, H., Loos, M., Meyer, L., Eds.; Cambridge University Press: Cambridge, U.K., 2005.
(5) Smit, B.; Reimer, J. R.; Oldenburg, C. M.; Bourg, I. C. *Introduction to Carbon Capture and Sequestration*; Imperial College Press: London, 2014.
(6) Neuzil, C. E. Can shale safely host U.S. nuclear waste? *EOS Trans. AGU* **2013**, *94*, 261−268.
(7) IEA. Gas to Coal Competition in the U.S. Power Sector. International Energy Agency, Organisation for Economic Co-operation and Development: Paris, 2013.
(8) Elliot, T. R.; Celia, M. A. Potential restrictions for CO_2 sequestration sites due to shale and tight gas production. *Environ. Sci. Technol.* **2012**, *46*, 4223−4227.
(9) Mazurek, M.; Alt-Epping, P.; Bath, A.; Gimmi, T.; Waber, H. N.; Buschaert, S.; De Cannière, P.; De Craen, M.; Gautschi, A.; Savoye, S.; Vinsot, A.; Wemaere, I.; Wouters, L. Natural tracer profiles across argillaceous formations. *Appl. Geochem.* **2011**, *26*, 1035−1064.
(10) NEA. Self-sealing of Fractures in Argillaceous Formations in the Context of Geological Disposal of Radioactive Waste. NEA Report 6184; Nuclear Energy Agency, Organization for Economic Co-operation and Development: Paris, 2010.
(11) Zoback, M. D.; Gorelick, S. M. Earthquake triggering and large-scale geologic storage of carbon dioxide. *Proc. Natl. Acad. Sci. U. S. A.* **2012**, *109*, 10164−10168.
(12) Jansen, T.; Zhu, D.; Hill, A. D. The effect of rock mechanical properties on fracture conductivity for shale formations. SPE Hydraulic Fracturing Technology Conference, Paper SPE-173347-MS; Society of Petroleum Engineers: Richardson, TX, 2015.
(13) Gutierrez, M.; Øino, L. E.; Nygård, R. Stress-dependent permeability of a de-mineralised fracture in shale. *Mar. Pet. Geol.* **2000**, *17*, 895−907.
(14) Kohli, A. H.; Zoback, M. D. Frictional properties of shale reservoir rocks. *J. Geophys. Res.* **2013**, *118*, 5109−5125.
(15) Bourg, I. C.; Beckingham, L. E.; DePaolo, D. J. The nanoscale basis of CO_2 trapping for geologic storage. *Environ. Sci. Technol.* **2015**, *49*, 10265−10284.
(16) Crawford, B. R.; Faulkner, D. R.; Rutter, E. H. Strength, porosity, and permeability development during hydrostatic and shear loading of synthetic quartz-clay fault gouge. *J. Geophys. Res.* **2008**, *113*, B03207.
(17) Wibberley, C. A. J.; Yielding, G.; Di Toro, G. Recent advances in the understanding of fault zone internal structure: a review. *Geol. Soc. Spec. Publ.* **2008**, *299*, 5−33.
(18) Manzocchi, T.; Childs, C.; Walsh, J. J. Faults and fault properties in hydrocarbon flow models. *Geofluids* **2010**, *10*, 94−113.
(19) Peltonen, C.; Marcussen, Ø.; Bjørlykke, K.; Jahren, J. Clay mineral diagenesis and quartz cementation in mudstones: The effects of smectite to Illite reaction on rock properties. *Mar. Pet. Geol.* **2009**, *26*, 887−898.
(20) Rinaldi, A. P.; Rutqvist, J.; Cappa, F. Geomechanical effects on CO_2 leakage through fault zones during large-scale underground injection. *Int. J. Greenhouse Gas Control* **2014**, *20*, 117−131.
(21) Carroll, S. A.; Keating, E.; Mansoor, K.; Dai, Z.; Sun, Y.; Trainor-Guitton, W.; Brown, C.; Bacon, D. Key factors for determining groundwater impacts due to leakage from geologic carbon sequestration reservoirs. *Int. J. Greenhouse Gas Control* **2014**, *29*, 153−168.
(22) Huang, X.; Bandilla, K. W.; Celia, M. A.; Bachu, S. Basin-scale modeling of CO_2 storage using models of varying complexity. *Int. J. Greenhouse Gas Control* **2014**, *20*, 73−86.
(23) Hillier, S. Appendix A. Mineralogical and chemical data. *Eng. Geol. Spec. Publ.* **2006**, *21*, 449−459.
(24) Robie, R. A.; Bethke, P. M.; Beardsley, K. M. Selected X-ray crystallographic data molar volumes, and densities of minerals and related substances. Geological Survey Bulletin 1248; U.S. Government Printing Office: Washington, DC, 1967.
(25) Dullien, F. A. L. *Porous Media. Fluid Transport and Pore Structure*, 2nd ed.; Academic Press: San Diego, 1992.
(26) Andreani, M.; Gouze, P.; Luquot, L.; Jouanna, P. Changes in seal capacity of fractured claystone caprocks induced by dissolved and gaseous CO_2 seepage. *Geophys. Res. Lett.* **2008**, *35*, L14404.
(27) Deng, H.; Ellis, B. R.; Peters, C. A.; Fitts, J. P.; Crandall, D.; Bromhal, G. S. Modifications of carbonate fracture hydrodynamic properties by CO_2-acidified brine flow. *Energy Fuels* **2013**, *27*, 4221−4231.
(28) Newell, D. L.; Carey, J. W. Experimental evaluation of wellbore integrity along the cement-rock boundary. *Environ. Sci. Technol.* **2013**, *47*, 276−282.
(29) Walsh, S. D. C.; Mason, H. E.; Du Frane, W. L.; Carroll, S. A. Mechanical and hydraulic coupling in cement-caprock interfaces exposed to carbonated brine. *Int. J. Greenhouse Gas Control* **2014**, *25*, 109−120.
(30) Tripathi, D.; Pournik, M. Effect of acid on productivity of fractured shale reservoirs. SPE/AAPG/SEG Unconventional Resources Technology Conference; Society of Petroleum Engineers: Richardson, TX, 2014.
(31) Kang, M.; Baik, E.; Miller, A. R.; Bandilla, K. W.; Celia, M. A. Effective permeabilities of abandoned oil and gas wells: Analysis of data from Pennsylvania. *Environ. Sci. Technol.* **2015**, *49*, 4757−4764.
(32) Gamage, K.; Screaton, E.; Bekins, B.; Aiello, I. Permeability-porosity relationships of subduction zone sediments. *Mar. Geol.* **2011**, *279*, 19−36.
(33) Schleicher, A. M.; Hofmann, H.; van der Pluijm, B. A. Constraining clay hydration state and its role in active fault systems. *Geochem. Geophys. Geosyst.* **2013**, *14*, 1039−1052.

DOI: 10.1021/acs.estlett.5b00233
Environ. Sci. Technol. Lett. 2015, 2, 255−259